BMC Research Notes

RESEARCH NOTE Open Access

CIRBP mRNA level in breast cancer is associated with HIF1α gene expression and microvascular density

Sajad Monjezi[1,4], Vahid Soleimani[2], Maryam Cheraghzadeh[1], Saeed Ghanbari[3] and Maryam Adelipour[1,4*]

Abstract

Objective Based on the available evidence, the cold-inducible RNA-binding protein (CIRBP) appears to play a role in increasing the stability of hypoxia-inducible factor 1-alpha (*HIF1α*) mRNA. This research aimed to examine the levels of *CIRBP* and *HIF1α* mRNA within breast tumor tissues and explore the relationship between their gene expression and tumor Microvascular density (MVD).

Results The results revealed a significant upregulation of *CIRBP (*5.07-fold) and *HIF1α* (4.5-fold) gene expression in BC samples compared to the surrounding normal tissues ($p < 0.001$). This upregulation was also associated with various clinicopathologic features. Furthermore, there was a correlation between *CIRBP* mRNA expression, *HIF1α* mRNA expression, and MVD. Consequently, this study suggests that *CIRBP* may have a role in promoting angiogenesis in BC.

Keywords Breast cancer, Microvascular density, Gene expression

Introduction

Breast cancer (BC) is currently considered the most common cancer in women, with 23.6 new cases per 100,000 [1]. In recent times, a multitude of research endeavors have been undertaken to pinpoint novel biomarkers facilitating early detection and treatment monitoring in BC [2–4]. Therefore, a deeper understanding of the fundamental mechanisms at play in BC can significantly contribute to the discovery of these new biomarkers. Angiogenesis, the formation of new blood vessels, is crucial for tumor growth and metastasis. Normally, it is regulated by a balance of pro-angiogenic and anti-angiogenic factors. In cancer, this balance is disrupted, leading to new blood vessel formation [5, 6]. Studies has shown that hypoxia-inducible factor 1α (HIF-1α) can directly stimulate the expression of specific angiogenic factors, such as vascular endothelial growth factor (VEGF), thus facilitating the formation of new blood vessels [7]. Notably, local hypoxia is known to occur during the early stages of BC development. In hypoxic conditions, there is a potential elevation in HIF-1α expression within tumor cells, subsequently promoting VEGF-induced angiogenesis [5]. It is important to emphasize the role of local hypoxia during the initial phases of breast cancer development, as it fosters a microenvironment that supports the upregulation of *HIF1α* and the subsequent induction of VEGF-mediated angiogenesis, which, in turn, drives tumor advancement, invasion, and metastasis [8].

*Correspondence:
Maryam Adelipour
adelimaryam@rocketmail.com; adelipour-m@ajums.ac.ir
[1]Department of Biochemistry, School of Medicine, Ahvaz Jundishapur University of Medical Sciences, Ahvaz, Iran
[2]Department of Pathology, School of Medicine, Cancer Institute, Tehran University of Medical Science, Tehran, Iran
[3]Department of Biostatistics and Epidemiology, School of Health, Ahvaz Jundishapur University of Medical Sciences, Ahvaz, Iran
[4]Cellular and molecular research center, Medical Basic Science Research Institute, Ahvaz Jundishapur University of Medical Sciences, Ahvaz, Iran

Furthermore, numerous studies have indicated that RNA-binding proteins, known for their role in governing RNA dynamics, have the capacity to influence angiogenesis [9]. Among these, Cold-inducible RNA-binding protein (*CIRBP*) belongs to the mammalian cold shock protein family and was initially identified in the testes. *CIRBP* is continuously expressed across various cell types and typically resides in the nucleus, though it can translocate to the cytoplasm under various cellular stressors like hypoxia, UV irradiation, and exposure to cold conditions [9–12]. Under such stressful circumstances, *CIRBP* can elevate its own expression through the activation of alternative promoters, a process known as self-transcription. Moreover, Specificity Protein 1 (SP1), acting as a transcriptional regulator, can bind to the 5' flanking region of the *CIRBP* gene and enhance *CIRBP* overexpression [10, 13]. In general, *CIRBP* binds to the 3'-untranslated region (UTR) of specific target genes, thereby regulating a wide spectrum of physiological and pathological events, including but not limited to cell survival, proliferation, differentiation, senescence, angiogenesis, apoptosis, and inflammatory responses [11, 12]. This multifaceted RNA-binding protein plays a pivotal role in response to stressors by orchestrating its own upregulation through alternative promoters, while the involvement of SP1 further amplifies its expression. Notably, evidence points to *CIRBP* having distinct roles in various human malignancies [14]. *CIRBP* has been found to be overexpressed in conditions like melanoma, prostate cancer, colorectal cancer, breast cancer, bladder cancer, and skin squamous cell carcinoma. However, in contrast, in cases of endometrial and ovarian cancer, *CIRBP* appears to act as a tumor suppressor [9, 15, 16].

Accumulating evidence indicates that *CIRBP* exhibits a selective affinity for the 3'-UTR sequence of *HIF1α* mRNA, leading to increased stability and enhanced translation of *HIF1α* mRNA. Prior research has proposed that *CIRBP* has the potential to induce the overexpression of HIF-1α in a variety of cancers, including bladder cancer [15]. However, the precise relationship between CIRBP and the angiogenesis process in BC is still unknown. Therefore, the primary objective of this study was to shed light on the role of angiogenesis in the proliferation and metastasis of breast tumor cells. To do this, we examined the mRNA expression levels of CIRBP and HIF1α, as well as MVD, in breast cancer tissues compared to the surrounding non-cancerous tissues.

Methods

Patient and tissue sample collection

We obtained 42 fresh-frozen tissue specimens from the Cancer Institute of Imam Khomeini Hospital in Tehran, following strict ethical guidelines. Non-tumor tissues adjacent to tumors were used as control samples. The sample size was determined using MedCalc statistical software, considering a statistical power of 90% ($\beta = 0.10$) and a significance level of 5% ($\alpha = 0.05$), which corresponds to the probability of committing a Type I error as described by Wang et al."To control for Type I error, we set the significance level at 5% ($\alpha = 0.05$), which is a commonly used threshold in biomedical research [17]. Demographic and tumor-specific data were collected. Patients had not undergone prior treatment and those with other cancer histories were excluded. All patients provided informed consent. Tumor size, grade, and stage were classified based on standard clinical and pathological guidelines. Tumor staging followed the TNM classification system established by the American Joint Committee on Cancer (AJCC), while tumor grading was assessed using histological criteria including nuclear pleomorphism, mitotic count, and glandular differentiation. All classifications were confirmed by experienced pathologists. The research followed the Helsinki Declaration and was approved by the Ethics Committee at Ahvaz Jundishapur University. Specimens were fresh-frozen and in liquid nitrogen and securely stored at -75°C for molecular experiments, adhering to STROBE guidelines [18].

RNA isolation and quantitative real-time PCR (qRT-PCR) analysis

To assess gene expression, total RNA was extracted from 42 BC tissues and their adjacent non-cancerous counterparts using RiboEx™ Reagent (Cat. No. 301-001, GeneAll Biotechnology, Seoul, Korea) as per the producer's guidelines. The quantity and integrity of the isolated RNA were validated employing a Nano Drop 2000 spectrophotometer (Thermo Scientific, USA) and 1.5% agarose gel electrophoresis. The next step complementary DNA (cDNA) was reverse transcripted by Yekta Tajhiz Azma Kit (Cat. No. YT4500, Tehran, Iran), following the kit's recommended protocol. To measure the expression levels of the *CIRBP* and HIF1 genes, quantitative real-time PCR (qRT-PCR) procedures were executed using an Applied BiosystemsTM 7500 Real-Time PCR System. Each PCR reaction (12.5 µl) was composed of 6.25 µL of RealQ Plus 2x Master Mix Green (Cat. No. A324402, Amplicon, Denmark), 0.5 µL each of forward and reverse primers (0.2 µM), 2 µL of template DNA, and 3.75 µL of RNase-free water. For data normalization, hypoxanthine phosphoribosyltransferase 1 (HPRT1) was utilized as a housekeeping gene. Specific forward and reverse primer sequences for CIRBP, HIF1α, and HPRT1 genes were obtained as follows: CIRBP Forward primer: AGGGCT GAGTTTTGACACCA, reverse primer: GCCGTCCAT CTACAGACTTCC; HIF1α Forward primer: GCAGCA ACGACACAGAAACT, reverse primer: TGCAGGGTC AGCACTACTT; HPRT1 Forward primer: CCTGGCGT CGTGATTAGTG, Reverse primer: TCAGTCCTGTCCA

TAATTAGTCC. In terms of the PCR cycle conditions, a total of 40 cycles were carried out, with each cycle involving a 15-second denaturation step at 95 °C followed by a 1-minute annealing step at 60 °C. This was preceded by an initial pre-incubation stage at 95 °C for 15 min. Furthermore, we assessed the melting curve by gradually increasing the temperature from 60 to 95 °C. The relative quantitative values (Fold Change) for each sample were calculated employing the $2^{-\Delta\Delta Ct}$ formula, with normalization to its respective housekeeping gene [19].

Immunohistochemical analysis

Immunohistochemistry analysis was carried out on thirty-nine paraffin-embedded tissue blocks originating from a pool of forty-two patients. In the case of BC tissues, they underwent fixation in 10% phosphate-buffered formalin before being embedded in paraffin. The 2.5 µm tissue sections underwent deparaffinization overnight in xylene and subsequent rehydration through a series of graded alcohol solutions. To suppress endogenous peroxidase activity, a solution of 3% H2O2-methanol was applied. To minimize non-specific staining, the sections were pre-treated with a 5% normal goat serum for a duration of 30 min. Following this, the sections were incubated overnight at 4 °C with primary antibodies (CD31, diluted to 1:25) (Cat. No. MAD-002048Q, Master Diagnostic, Spain). A subsequent 60-minute incubation with secondary antibodies (MAD-000237QK) followed. The resulting immunoreaction product was visualized through diaminobenzidine staining, and the slides were counterstained with hematoxylin. The examination of tissue sections was conducted using a light microscope. In our study, about ten fields were randomly chosen and examined at 40X magnification, with the resulting mean vessel count calculated across these ten fields [20, 21].

Statistical analysis

Statistical analyses were conducted using GraphPad Prism and SPSS software. Data were presented as Mean ± standard deviation (SD) from at least three independent experiments. Normality was assessed with the Kolmogorov–Smirnov test, and significance was set at $p < 0.05$. Gene expression between two groups of tumor tissues and control was compared using paired sample t-test. ROC analysis evaluated gene sensitivity and specificity as biomarkers. Pearson correlation coefficient test assessed correlations between CIRBP and HIF1α transcription and their expression with MVD. Comparisons involving clinicopathological factors were made as follows: Independent sample t-test was used for tumor size (< 5 cm vs. ≥ 5 cm), ER status (positive vs. negative), PR status (positive vs. negative), P53 status (positive vs. negative), necrosis (yes vs. no), lymphatic invasion (yes vs. no), vascular invasion (yes vs. no), and stage (II, III). One-way ANOVA was used for tumor grade (I, II, III), Bonferroni correction was applied to adjust the significance level (α) for multiple comparisons. The adjusted significance level was calculated as α, where ensuring a more stringent control of Type I error [20, 22].

Results

Clinicopathological characteristics of patients

Demographic characteristics and clinical pathology of the 42 BC patients revealed that 58% were under 50 years old, while 42% were 50 or older. Additionally, 30.5% of patients were of Azeri ethnicity. The data showed that approximately 71.4% of patients were at stage II, and 47.6% were classified as grade II.Necrosis was present in 64.3% of cases, and vascular/lymphatic invasion was observed in 61.9% of patients. Tumor size analysis indicated that 54.8% of patients had tumors smaller than 5 cm, while 45.2% had tumors 5 cm or larger.

CIRBP and HIF1α expression levels in breast cancer specimens

The QRT-PCR method was employed to assess the mRNA expression of *CIRBP* and *HIF1α* genes in 42 BC tissues as well as their corresponding normal adjacent breast tissues. It was evident that the transcript levels of both *CIRBP* and *HIF1α* genes exhibited a noteworthy increase in BC tissues when compared to the adjacent normal tissues ($P < 0.001$). Specifically, *CIRBP* and *HIF1α* transcripts experienced a substantial upsurge of approximately 5.07-fold and 4.5-fold, respectively, in BC samples as opposed to normal samples ($P < 0.001$), as visually depicted in Fig. 1.

Association between CIRBP and HIF1α mRNA levels and clinicopathological features of patients

Table 1 outlines the findings regarding the correlation between CIRBP mRNA levels and various clinicopathological parameters in BC patients. Our data analysis by independent sample t-test or one way ANOVA unveiled significant associations between elevated *CIRBP* transcript levels and several clinical parameters, including tumor size ($P = 0.016$), grade ($P<0.001$), stage ($P = 0.018$), necrosis ($P = 0.045$), lymphatic invasion ($P = 0.008$), and vascular invasion ($P = 0.008$). Notably, *CIRBP* mRNA levels did not demonstrate a significant correlation with other histopathological markers, such as p53, estrogen receptor (ER), and progesterone receptor (PR) (P˃0.05, as indicated in Table 1.

As for relationship of *HIF1α* mRNA expression and the clinicopathological characteristics of BC tissues, the analysis of data by independent sample t-test or one way ANOVA revealed significant disparities in *HIF1α* gene transcript levels concerning tumor size ($P = 0.015$), grade ($P = 0.027$), stage ($P = 0.002$), lymphatic invasion

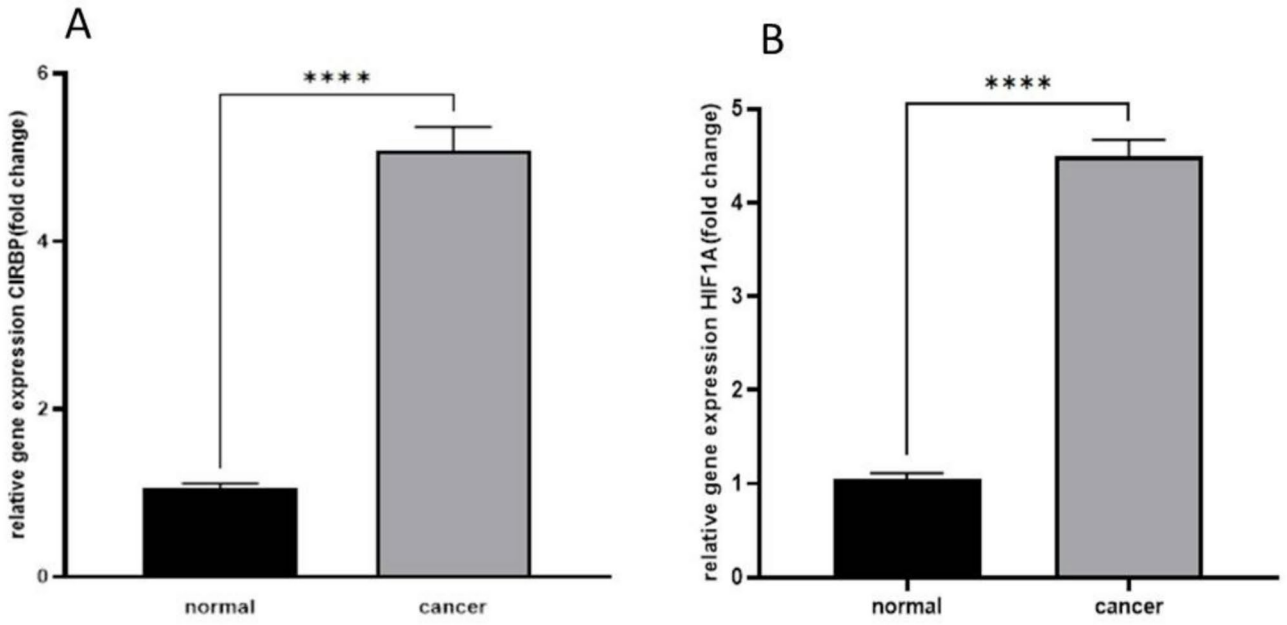

Fig. 1 Expression of CIRBP and HIF1 α gene in breast tumor tissues and no-tumor tissues. (**A**) Graph is showing the mRNA level of CIRBP in breast tumor tissues in compression with non-tumor tissues. (**B**) Graph is showing the mRNA level of HIF1α in breast tumor tissues in compression with non-tumor tissues. Data were expressed as mean ± standard deviation (SD). HPRT1 was used as a housekeeping gene. $^{****}P < 0.0001$ was compared to the normal group—BC = Breast cancer, CIRBP = Cold-inducible RNA-binding protein, HIF1α = Hypoxia-inducible factor 1α, HPRT1 = Hypoxanthine phosphoribosyltransferase1

($P = 0.012$), and vascular invasion ($P = 0.012$). However, it's worth noting that the *HIF1α* mRNA levels did not exhibit a significant correlation with other clinicopathological features.

Correlation between the transcriptional levels of CIRBP and HIF1α genes

Within BC tissues and their adjacent normal counterparts, a statistically moderate positive correlation was observed (correlation coefficient (r) = 0.362, $P = 0.018$) between the normalized expression levels of the *CIRBP* and *HIF1α* genes. These results suggest that an escalation in *CIRBP* expression may indeed play a role in bolstering the stability and subsequent overexpression of the *HIF1α* gene [23, 24].

MVD evaluation

In Fig. 2, the depiction showcases the density of blood vessels, visually represented by distinct brown dots. The samples have been stratified into categories, distinguishing them as exhibiting low, moderate, or high levels of MVD. Interestingly, we observed that lower CD31 expression levels were evident in the context of grades I and II within BC tissues. In contrast, a pronounced abundance of vessel lumens, as indicated by CD31, was detected in grade III specimens.

Correlation between MVD and clinicopathological features of patients

Table 2 highlights a substantial association between MVD and the clinicopathological characteristics of patients, specifically tumor size, grade, and stage. With an increase in the size ($P = 0.005$), grade ($P = 0.033$), and stage ($P = 0.002$) of the tumor cells, there was a corresponding escalation in MVD induced by these tumor cells. Nonetheless, it's noteworthy that the MVD did not exhibit a significant correlation with other clinicopathological patient features, including the status of ER, PR, HER2 receptor, p53, necrosis, and vascular-lymphatic invasion.

Correlation between MVD with CIRBP and HIF1α transcriptional levels

Within BC tissues and their corresponding normal tissue counterparts, an intriguing observation emerged. A weak negative correlation was unveiled (R=-0.326, $P = 0.035$) between the ΔCT value of the *CIRBP* gene and MVD. This finding suggests that a decrease in the ΔCT value of the CIRBP gene may be associated with an increase in MVD rates. However, it's important to note that the statistical analysis failed to reveal a significant relationship between *HIF1α* gene expression and the MVD rate ($R = 0.052$, $P = 0.745$).

Table 1 Association of CIRBP and HIF1α expression with clinicopathological features

Variables	CIRBP		HIF1α	
	Mean fold change(± SD)	*p*-value	Mean fold change(± SD)	*p*-value
Tumor size (cm)				
< 5	4.213(± 0.295)	**0.016***	4.027(± 0.229)	**0.015***
≥ 5	5.646 (± 0.485)		4.855 (± 0.223)	
Grade				
I	3.659(± 0.450)	**<0.001***	3.871(± 0.337)	**0.027***
II	4.276(± 0.362)		4.290(± 0.222)	
III	6.585(± 0.495)		5.075(0.296)	
Stage				
II	4.534(± 0.322)	**0.018***	4.174(± 0.183)	**0.002***
III	6.158(± 0.660)		5.317(± 0.276)	
ER				
Positive	5.429(± 0.407)	0.097	4.611(± 0.231)	0.660
Negative	4.364(± 0.467)		4.337(± 0255)	
PR				
Positive	5.464(± 0.432)	0.104	4.698(± 0.216)	0.208
Negative	4.434(± 0.435)		4.693(± 0.214)	
P53				
Positive	4.420(± 0.573)	0.152	4.187(0.275)	0.154
Negative	5.354(± 0.357)		4.693(± 0.214)	
Necrosis				
Yes	5.406(± 0.437)	**0.045***	4.692(± 0.225)	0.135
No	4.264(± 0.334)		4.154(± 0.240)	
Lymphatic invasion				
Yes	5.639(± 0.412)	**0.008***	4.830(± 0.223)	**0.012***
No	3.956(± 0.365)		3.964(0.211)	
Vascular invasion				
Yes	5.639(± 0.412)	**0.008***	4.830(± 0.223)	**0.012***
No	3.956(± 0.365)		3.964(0.211)	

ER = estrogen receptor, PR = progesterone receptor, CIRBP = Cold-inducible RNA-binding protein, HIF1α = Hypoxia-inducible factor 1α

Fold change = describes the ratio of two values, e.g. (gene expression in condition 1)/(gene or variable expression in condition 2)

* Indicates a significant difference

Sensitivity and specificity of CIRBP and HIF1α as biomarkers

The ROC curve was used to evaluate the specificity and sensitivity of the CIRBP and HIF1α genes. The area under the curve (AUC) for CIRBP was 89% ($P < 0.001$), while for HIF1α it was 91.7% ($P < 0.001$). With a cut-off of 1.40, CIRBP demonstrated a sensitivity of 93% and a specificity of 75%. In contrast, HIF1α, with a cut-off of 2.60, showed a sensitivity of 86% and a specificity of 91.7%, as illustrated in Fig. 3.

Discussion

Given the critical role of CIRBP in cancer biology, our study focused on its expression in breast cancer, along with HIF1α and MVD levels, using RT-qPCR and immunohistochemistry (IHC) analyses. Our results unequivocally showed that *CIRBP* mRNA expression exhibited a marked elevation in BC tissues when compared to their corresponding noncancerous counterparts. Additionally, our findings shed light on the fact that heightened *CIRBP* expression was significantly linked to larger tumor size, higher grade, advanced stage, and the presence of lymphatic/vascular invasion. These observations align with the findings of certain prior studies, which have reported instances of *CIRBP* overexpression particularly in hypoxic conditions [25]. Hence, the hypoxic environment commonly found in solid tumors may plausibly contribute to the heightened expression of CIRBP in breast tumor tissues. This observation is supported by Zhou et al., who reported CIRBP upregulation in renal cell carcinoma tissues compared to non-cancerous tissues. They found a notably positive CIRBP expression in 76.5% of tumor samples, as opposed to adjacent non-tumor tissues, using IHC [26]. Furthermore, our research outcomes displayed disparities when compared to the dynamics of *CIRBP* in certain other cancer types. For instance, in the case of ovarian cancer, the work of Zou et al. presented a contrasting scenario wherein both mRNA and protein levels of *CIRBP* exhibited significant reduction in ovarian cancer tissues in contrast to normal tissues. Their mechanistic analysis unveiled that the knockdown of *CIRBP* led to the suppression of apoptosis, while simultaneously inducing cell proliferation and metastasis in ovarian cancer cells. Additionally, they reported that *CIRBP* had the capability to bind to the Mitogen-Activated Protein Kinase (MAP2K) gene, thereby bolstering its stability. As per the insights from Zou's study, it appears that one of the roles assumed by CIRBP as a tumor suppressor in ovarian cancer stems from its influence on MAP2K stability [16]. Roilo et al. provided compelling evidence for the tumor suppressor role of *CIRBP*, highlighting its capability to interact with the 5'-UTR of p27kip1 mRNA, consequently enhancing its stability [24]. Roilo's findings diverge from our own, potentially attributed to the examination of *CIRBP* under distinct conditions. It's vital to recognize that in vitro data may not precisely mirror in vivo conditions. Considering these observations, CIRBP and HIF1α may serve as promising predictive biomarkers, and their roles in tumor progression suggest they could be explored as potential therapeutic targets, particularly in the context of small molecule inhibitors [27].

Given the established role of CIRBP in cellular stress responses, some studies have reported a connection between CIRBP and HIF1α, highlighting their potential interaction in hypoxia. The study of Lu et al., revealed that CIRBP upregulation possessed the capacity to enhance *HIF1α* expression in bladder cancer cells. Conversely, the transfection of cells with siRNA targeting *CIRBP* led to a reduction in *HIF1α* expression. These

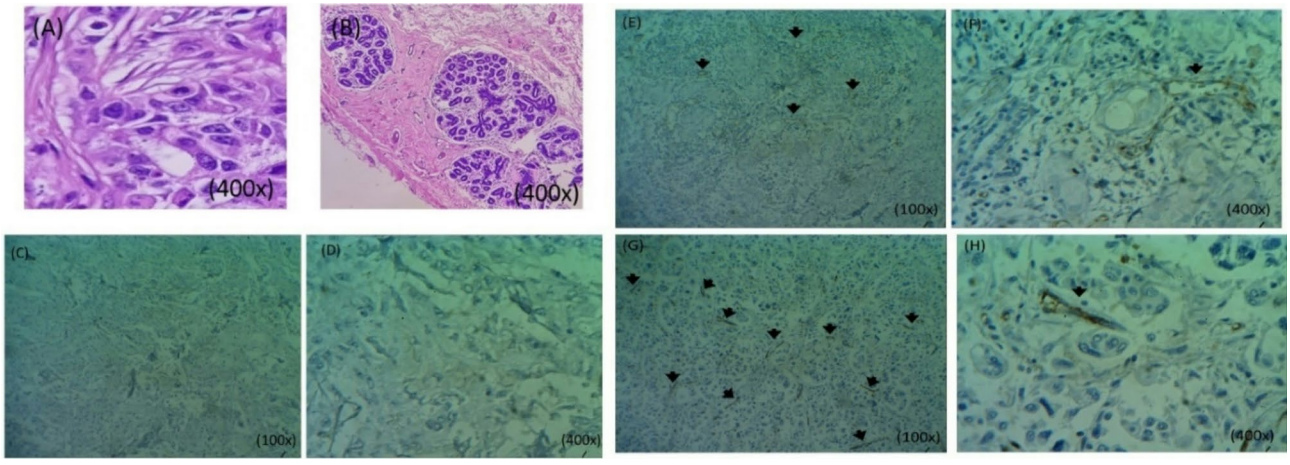

Fig. 2 Microvessel density in breast tumor tissue. (**A**) A pathological image of breast cancer (**B**) A normal image of breast cancer (**C**) Lack of expression of CD31 in (BC) samples (100X) and (**D**) (400X). (**E**) Low level of CD31 expression in grade I of (BC) samples (100X) and (**F**) (400X). (**G**) High level of CD31 expression in grade III of (BC)samples (100X) and (**H**) (400X)

Table 2 Evaluation of MVD rate with clinicopathological features of breast cancer patients

Variables	Mean of hot spot/mm2 ± SD	*p*-value
Tumor size (cm)		
< 5	3.157.(± 0.617)	**0.005***
≥ 5	8.478 (± 1.612)	
Grade		
I	4.142(± 2.482)	**0.033***
II	4.150(± 0.932)	
III	9.533(± 2.037)	
Stage		
II	5.533(± 1.058)	**0.002***
III	7.416(± 2.359)	
HER2		
Positive	8.647(± 2.003)	0.060
Negative	4.320(± 0.875)	
ER		
Positive	6.320(± 1.376)	0.768
Negative	5.705(± 1.484)	
PR		
Positive	6.391(± 1.444)	0.731
Negative	5.682(± 1.410)	
P53		
Positive	4.066(± 1.093)	0.139
Negative	7.185(± 1.410)	
Necrosis		
Yes	7.333(± 1.367)	0.060
No	3.800(± 1.211)	
Lymphatic/Vascular invasion		
Yes	7.038(± 1.367)	0.224
No	4.500(1.387)	

* indicates a significant difference

observations were underpinned by *CIRBP's* ability to bind to the 3'-UTR of HIF-1α mRNA, consequently bolstering the stability of the transcript and facilitating its translation in the context of bladder cancer [15]. In line with the study by Lu et al., our research further corroborated the relationship between CIRBP and HIF1α. We demonstrated that increased CIRBP expression correlated with enhanced HIF1α expression in tumor tissues. These findings reinforce the notion that CIRBP plays a pivotal role in regulating HIF1α expression levels, potentially through mechanisms such as direct binding to the 3'-UTR of HIF1α mRNA, as observed in bladder cancer cells. The study by Zhang et al. supports these findings by suggesting a mechanism in which CIRP (cold-inducible RNA-binding protein) knockout diminishes HIF1α expression in a rat model of renal ischemia-reperfusion injury. They proposed that CIRP knockout upregulates rat Phd3 expression, a critical regulator of HIF-1α. In parallel, experiments in HK-2 cells revealed that this upregulation inhibits HIF-1α following deep hypothermic circulatory arrest (DHCA), potentially initiating ROS-TGF-β1/p38 MAPK activation and mitochondrial apoptotic pathways [28]. Several studies have documented the overexpression of the *HIF1α* gene in various cancer types. Kaya et al., for instance, noted that heightened levels of *HIF1α* expression were correlated with the presence of HER-2 expression in HER2-positive patients, as well as in patients lacking ER and PR expression [29]. Our research findings revealed that elevated HIF1α expression was significantly associated with larger tumor size, the presence of necrosis, and a lower incidence of lymphatic and vascular invasion. These findings exhibited a striking parallel with outcomes in endometrial cancer. In a study by Fuzi et al., the mRNA expression levels of *HIF1α* in endometrial cancer tissues were compared to normal endometrium samples, revealing that heightened *HIF1α* expression played a promotive role in tumorigenesis. Furthermore, the application of RNA interference (RNAi) for *HIF1α* knockdown effectively curtailed the proliferation of the endometrial cancer cell line HEC-1 A

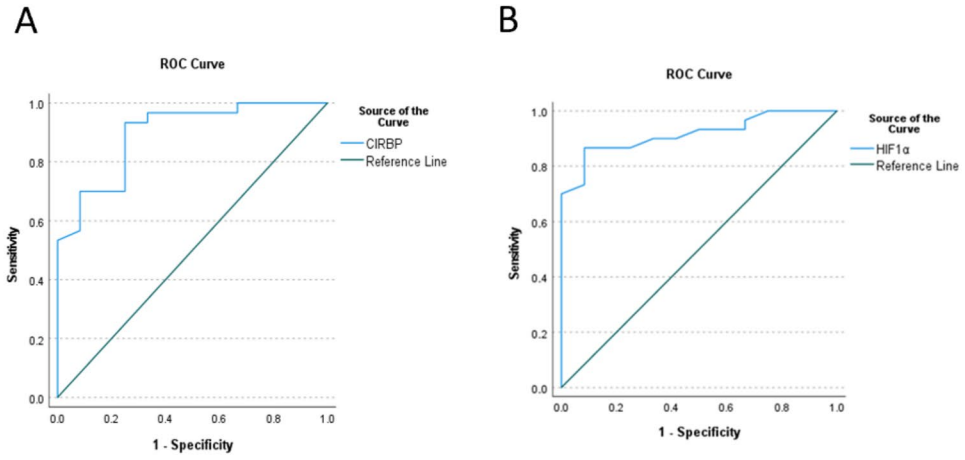

C

ROC Curve Analyses for Evaluation of the Diagnostic Power of CIRBP and HIF1α in Patients with breast cancer

GOI	AUC (%)	P–Value	cut–off point	Sensitivity	Specificity
CIRBP	89%	0.001*	1.4	93%	75%
HIF1α	91.7	0.001*	2.6	86%	91.7%

Abbreviations: GOI, gene of interest; AUC, area under the curve; *P-value less than 0.05 was considered significant

Fig. 3 ROC curve analysis of CIRBP and HIF1α genes. (**A**) ROC curve of CIRBP gene (**B**) ROC curve of HIF1α gene. (**C**) ROC curve analysis CIRBP and HIF1α CIRBP = Cold-inducible RNA-binding protein, HIF1α = Hypoxia-inducible factor 1α

[30]. Consequently, the heightened presence of *HIF1α* within cancer cells emerges as a potential driver of malignancy, positioning it as an oncogene.

The primary objective of our study revolved around the assessment of MVD in BC tissues, with a specific focus on its correlation with clinicopathological characteristics and the expression of *CIRBP* and *HIF1α*. Our findings compellingly illustrated a substantial association between the MVD rate and critical parameters including tumor size, grade, and stage. This discovery aligns with a study by Krishnapriya et al., who conducted an examination of the MVD rate in advanced BC biopsies from 92 patients, ultimately concluding that MVD was significantly elevated in BC tissues when compared to normal breast tissues. Furthermore, they provided insight into the prognostic potential of MVD by establishing a link between higher MVD and shorter survival periods in BC, thereby advocating for the consideration of MVD as a valuable prognostic marker [31]. In a separate investigation, Agnani et al. identified a notable association between MVD rate and various crucial factors including tumor size, lymph node metastasis, lymphovascular invasion, and tumor grade within the context of invasive ductal carcinoma [32]. Our results further suggest a moderate negative correlation between CIRBP mRNA expression and MVD. Considering that a lower Ct value indicates higher gene expression, it suggests that an increase in gene expression of CIRBP is associated with an increase MVD. Intriguingly, the data unveiled a lack of significant correlation between *HIF1α* mRNA expression and MVD. This outcome deviates from the conclusions drawn in prior studies [33], possibly influenced in part by the relatively limited number of patients studied and the diminished quality of paraffin blocks housing BC tissues subjected to extended storage periods. In addition, our analysis encompassed an evaluation of the sensitivity and specificity of *CIRBP* and *HIF1α* genes, culminating in the identification of high values, specifically 93% and 75% for *CIRBP*, and 86% and 91.7% for *HIF1α*, respectively. These remarkable metrics underscore the potential utility of these genes as biomarkers for distinguishing BC tissue from non-cancerous tissue. Nonetheless, it is imperative to acknowledge the inherent limitations within our study. These limitations encompassed the unavailability of patient survival data, which precluded the determination of the role these genes might play in disease prognosis.

Additionally, our capacity to measure protein levels of *CIRBP* and *HIF1α* was constrained, and the exploration of the interaction between *CIRBP* and *HIF1α* remained unexplored within an in vitro system.

Conclusion

This study has revealed that CIRBP and HIF1α gene expression is significantly higher in breast cancer tissues compared to non-cancerous tissues. These findings suggest that these genes may serve as potential biomarkers for distinguishing between cancerous and non-cancerous tissues. However, further studies are needed to establish the prognostic role of CIRBP expression in breast cancer. The increased expression of CIRBP and HIF1α in higher-grade tumors indicates that these genes might also serve as prognostic markers. Additionally, the correlation between CIRBP expression and MVD suggests its potential role in tumor angiogenesis. Understanding these mechanisms could aid in the development of targeted cancer therapies.

Acknowledgements
This article constitutes a part of Sajad Monjezi's master dissertation at Ahvaz Jundishapur University of Medical Sciences. The authors wish to extend their heartfelt appreciation to the entire team and mentors at Ahvaz Jundishapur University of Medical Sciences for their valuable contributions to this research.

Author contributions
S.M. and M.A. contributed to design of the research; S.M., M.A., V.S., S.G. and M.C. collected the data; S.M. and M.A. contributed to interpretation of the data; S.M. wrote the main manuscript; M.A. revised the manuscript. All authors read and approved the final manuscript.

Funding
This study was financially supported Ahvaz Jundishapur University of Medical Sciences (grant number: CMRC-0050).

Data availability
No datasets were generated or analysed during the current study.

Declarations

Ethical approval and consent to participate
This study was performed in accordance with the principles of the Declaration of Helsinki. All patients of have declared their informed consent through a written consent letter to be involved in this study. This study is approved by the ethics committee of the cancer institute of Imam Khomeini hospital (Tehran, Iran) and the ethics committee of Ahvaz Jundishapour University of medical sciences (Ahvaz, Iran) (IR.AJUMS.MEDICINE.REC. 1400.052).

Consent for publication
Not applicable.

Competing interests
The authors declare no competing interests.

Conflict of interest
The authors declared no conflicts of interest.

Received: 7 March 2025 / Accepted: 23 April 2025
Published online: 04 May 2025

References

1. Farhood B, Geraily G, Alizadeh A. Incidence and mortality of various cancers in Iran and compare to other countries: a review Article. Iran J Public Health. 2018;47(3):309.
2. Wu M, Li Q, Wang H. Identification of novel biomarkers associated with the prognosis and potential pathogenesis of breast cancer via integrated bioinformatics analysis. Technol Cancer Res Treat. 2021;20:1533033821992081.
3. Mishra D, Mishra A, Rai SN, Vamanu E, Singh MP. Identification of prognostic biomarkers for suppressing tumorigenesis and metastasis of hepatocellular carcinoma through transcriptome analysis. Diagnostics 2023.13(5): 965.
4. Mishra D, Mishra A, Nand Rai S, Vamanu E, P Singh M. Demystifying the role of prognostic biomarkers in breast cancer through integrated transcriptome and pathway enrichment analyses. Diagnostics. 2023;13(6):1142.
5. de Heer EC, Jalving M, Harris AL. HIFs, angiogenesis, and metabolism: elusive enemies in breast cancer. J Clin Investig. 2020;130(10):5074–87.
6. Madu CO, Wang S, Madu CO, Lu Y. Angiogenesis in breast cancer progression, diagnosis, and treatment. J Cancer. 2020;11(15):4474.
7. Tirpe AA, Gulei D, Ciortea SM, Crivii C, Berindan-Neagoe I. Hypoxia: overview on hypoxia-mediated mechanisms with a focus on the role of HIF genes. Int J Mol Sci. 2019;20(24):6140.
8. Zarychta E, Ruszkowska-Ciastek B. Cooperation between angiogenesis, vasculogenesis, chemotaxis, and coagulation in breast cancer metastases development: pathophysiological point of view. Biomedicines. 2022;10(2):300.
9. Kim Y-M, Hong S. Controversial roles of cold–inducible RNA–binding protein in human cancer. Int J Oncol. 2021;59(5):1–11.
10. Liao Y, Tong L, Tang L, Wu S. The role of cold-inducible RNA binding protein in cell stress response. Int J Cancer. 2017;141(11):2164–73.
11. Qin H, Ni H, Liu Y, Yuan Y, Xi T, Li X, Zheng L. RNA-binding proteins in tumor progression. J Hematol Oncol. 2020;13(1):1–23.
12. Zhong P, Huang H. Recent progress in the research of cold-inducible RNA-binding protein. Future Sci OA. 2017;3(4):FSO246.
13. Kim SY, Ban H-J, Lee S. Jin. Regulation of CIRP by genetic factors of SP1 related to cold sensitivity. Front Immunol. 2022;13:994699.
14. Lujan DA, Ochoa JL, Hartley RS. Cold-inducible RNA binding protein in cancer and inflammation. Wiley Interdisciplinary Reviews: RNA. 2018;9(2):e1462.
15. Lu M, Ge Q, Wang G, Luo Y, Wang X, Jiang W, Liu X, Wu C-L, Xiao Y, Wang X. CIRBP is a novel oncogene in human bladder cancer inducing expression of HIF-1α. Cell death & disease. 2018.9(10): 1–15.
16. Zou D, Wang D, Zhou Q, Yu J. Downregulation of RNA binding protein CIRBP (cold-inducible RNA-binding protein) promotes ovarian cancer progression by regulating MAP2K4 mRNA stability and translation. Gynecol Oncol. 2019;154:66.
17. Wang M, Zhang H, Heng X, Pang Q, Sun A. Expression of cold-inducible RNA-binding protein (CIRP) in pituitary adenoma and its relationships with tumor recurrence. Med Sci Monitor: Int Med J Experimental Clin Res. 2015;21:1256.
18. von Elm ME, Altman DG, Egger M, Pocock SJ, Gøtzsche PC, Vandenbroucke JP. The strengthening the reporting of observational studies in epidemiology (STROBE) statement: guidelines for reporting observational studies. Ann Intern Med. 2007;147(8):573.
19. Moazeni-Roodi A, Allameh A, Harirchi I, Motiee-Langroudi M, Garajei A. Studies on the contribution of Cox-2 expression in the progression of oral squamous cell carcinoma and H-Ras activation. Pathol Oncol Res. 2017;23(2):355–60.
20. Mohammed RA, Ellis IO, Mahmmod AM, Hawkes EC, Green AR, Rakha EA, Martin SG. Lymphatic and blood vessels in basal and triple-negative breast cancers: characteristics and prognostic significance. Mod Pathol. 2011;24(6):774–85.
21. Weidner N. Current pathologic methods for measuring intratumoral microvessel density within breast carcinoma and other solid tumors. Breast Cancer Res Treat. 1995;36(2):169–80.
22. Ahani M, Ghaderian SMH, Azma MM, Kamali K, Gargari BN, Vojdani S. Association of STAT3, PTPRT, TNK2-AS1, LINC-ROR genes expression level with prostate Cancer and benign prostatic hyperplasia. Int J Cancer Manage 2022.15(1).
23. Juan Y, Haiqiao W, Xie W, Huaping H, Zhong H, Xiangdong Z, Kolosov VP, Perelman JM. Cold-inducible RNA-binding protein mediates airway inflammation and mucus hypersecretion through a post-transcriptional regulatory mechanism under cold stress. Int J Biochem Cell Biol. 2016;78:335–48.
24. Roilo M, Kullmann MK, Hengst L. Cold-inducible RNA-binding protein (CIRP) induces translation of the cell-cycle inhibitor p27Kip1. Nucleic Acids Res. 2018;46(6):3198–210.

25. Wellmann S, Bührer C, Moderegger E, Zelmer A, Kirschner R, Koehne P, Fujita J, Seeger K. Oxygen-regulated expression of the RNA-binding proteins RBM3 and CIRP by a HIF-1-independent mechanism. J Cell Sci. 2004;117(9):1785–94.
26. Zhou KW, Jiang K, Zhu W, Weng G. Expression of cold–inducible RNA–binding protein (CIRP) in renal cell carcinoma and the effect of CIRP downregulation cell proliferation and chemosensitivity to gemcitabine. Oncol Lett. 2018;15(5):7611–6.
27. Thumpati P, Rai SN, Prajapati C, Ramakrishna K, Singh SK. Targeting c-MYC G-Quadruplexes for Cancer treatment with small molecules. Sci Pharm. 2025;93(1):6.
28. Zhang P, Bai L, Tong Y, Guo S, Lu W, Yuan Y, Wang W, Jin Y, Gao P, Liu J. CIRP attenuates acute kidney injury after hypothermic cardiovascular surgery by inhibiting PHD3/HIF-1α-mediated ROS-TGF-β1/p38 MAPK activation and mitochondrial apoptotic pathways. Mol Med. 2023;29(1):61.
29. Kaya A, Gunel N, Benekli M, Akyurek N, Buyukberber S, Tatli H, Coskun U, Yildiz R, Yaman E. Ozturk. Hypoxia inducible factor-1 alpha and carbonic anhydrase IX overexpression are associated with poor survival in breast cancer patients. J Buon. 2012;17(4):663–8.
30. Fuzi AAM, Omar SZ, Mohamed Z, Adenan NAM, Mokhtar NM. High throughput Silencing identifies novel genes in endometrioid endometrial cancer. Taiwan J Obstet Gynecol. 2018;57(2):217–26.
31. Krishnapriya S, Malipatil B, Surekha S, Sundersingh S, Sridevi V, Ananthi B, Selvaluxmy G, Ganesan TS. Microvessel density (MVD) in locally advanced breast cancer. Asian Pac J Cancer Prevention: APJCP. 2019;20(5):1537.
32. Agnani B, Solanki R, Ansari M, Agnani S. Prognostic significance of microvessel density as assessed by anti CD34 monoclonal antibody in invasive ductal carcinoma of breast. Asian Pac J Cancer Biology. 2020;5(3):75–9.
33. Cui W, Xiao Y, Zhang R, Zhao N, Zhang X, Wang F, Liu Y, Zhang X, Hao J. SOHLH2 suppresses angiogenesis by downregulating HIF1α expression in breast Cancer. Mol Cancer Res. 2021;19(9):1498–509.

Publisher's note